Journal of Molecular Catalysis A: Chemical 349 (2011) 36–41

Contents lists available at SciVerse ScienceDirect

Journal of Molecular Catalysis A: Chemical

journal homepage: www.elsevier.com/locate/molcata

Solar-light induced photodegradation of organic pollutants over CdS-pillared zirconium–titanium phosphate (ZTP)

D.P. Das*, Niranjan Biswal, Satyabadi Martha, K.M. Parida*

Colloids and Materials Chemistry Department, CSIR-Institute of Minerals and Materials Technology, Bhubaneswar 751 013, Orissa, India

ARTICLE INFO

Article history:
Received 21 February 2011
Received in revised form 10 August 2011
Accepted 16 August 2011
Available online 22 August 2011

Keywords:
CdS-pillared zirconium–titanium phosphate
Methylene blue
Band gap energy
leuco-Methylene blue

ABSTRACT

With an attempt to extend the light absorption towards visible range and inhibit the rapid recombination of excited electrons and holes during photoreaction, a new type of photocatalysts, cadmium sulfide pillared zirconium–titanium phosphate (CdS-ZTP) powders were synthesised by two step sulfurisation route. The photocatalysts were characterised by SAXS, N_2 adsorption–desorption, DRUV–vis, PL, SEM/EDX, XPS, TPD and photocurrent measurements. The samples exhibited a unique property of optical absorption in UV and visible region with a wave length, $\lambda \leq 450$ nm followed by a clear long tail up to 700 nm. CdS pillaring has increased the photocatalytic efficiency of ZTP by three folds by increasing surface area, visible light sensitivity and decreasing band gap energy to 2.81 eV. The pillared materials showed excellent activity towards degradation of organic pollutants under solar light illumination. Amongst all the photocatalysts, 15CdS-ZTP showed the best photoactivity in the range of 70–94% and 64% towards the degradation of textile dyes and phenol, respectively in 180 min.

1. Introduction

The development of visible light responsive semiconducting materials has become one of the most challenging topics today for effective utilization of solar radiation. Numerous research attempts are recently being implemented to tune the band gap of the semiconducting material; by doping with transition metal cations [1–5], by creating oxygen vacancies [6] and more recently, by replacing lattice oxygen with B, C, N or S dopants [7–12]. But, scanty literatures are available on visible light driven photocatalysts [13–15]. Amongst all the visible light active materials, CdS is one of the active catalyst having suitable band gap, 2.4 eV which matches well with the solar spectrum. The instability to photooxidation of lattice is partially due to the ionic character of this semiconductor which means that the valence band is derived primarily from S 3p orbitals and the conduction band from Cd 5s orbital. CdS readily photodegrades, releasing toxic Cd^{2+} ions upon illumination which is called photocorrosion [16,17]. Therefore, continuous attempts have been made by the esteem researchers to improve the stability of metal sulfide by e.g. immobilizing CdS particles, coupling with another semiconductor with wide band gap [18,19] or intercalating metal sulfides into the layers of a semiconducting material [20–24].

Recently, Kapoor et al. reported the preparation of mesoporous zirconium–titanium phosphates (ZTPs) with a range of compositions [25]. The material showed improved ion-exchange properties and selectivity for particular metal ions in comparison with single salt counterparts. Hence, this can be a good support for CdS. Till date, up to the best of our knowledge first ever report on CdS pillared ZTP was reported by our group for water splitting under visible light illumination [23].

The present investigation reports the application of CdS pillared zirconium–titanium phosphate catalyst towards degradation of organic contaminants under solar light illumination. The high photocatalytic activity of the novel pillared materials has been correlated with various surface and textural characteristics.

2. Experimental

The preparation of *x*CdS-ZTP was reported elsewhere [23] and characterized by SAXS, DRUV–vis, PL, N_2 adsorption–desorption studies, SEM-EDS, TPD analyses, XPS and photocurrent measurement. Small angle X-ray diffraction patterns were recorded on a Rigaku Miniflex (set at 30 kV and 15 mA) powder diffractometer using Cu Kα radiation within the 2θ range from 1 to 10° at a rate of 2°/min in steps of 0.01°. N_2 adsorption–desorption studies were carried out by ASAP 2020 (Micromeritics) instrument at a liquid nitrogen temperature (−196 °C). Prior to analysis, the particles were subjected to vacuum (10^{-5} Torr) at 110 °C for 5 h to ensure a clean surface. Surface area was calculated with Brunauer–Emmett–Teller (BET) method using the adsorption data

* Corresponding authors. Tel.: +91 674 2379425; fax: +91 674 2379137.
E-mail addresses: das_dipti77@yahoo.co.in (D.P. Das), paridakulamani@yahoo.com (K.M. Parida).

1381-1169/$ – see front matter © 2011 Elsevier B.V. All rights reserved.
doi:10.1016/j.molcata.2011.08.012

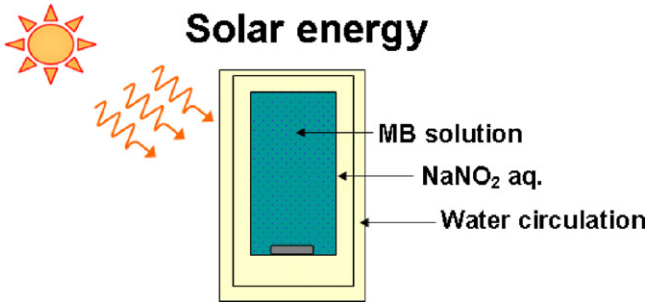

Scheme 1. Schematic representation of reaction set up.

within the p/p^0 range from 0.05 to 0.33. The pore volume was measured at a relative pressure p/p^0 of 0.95. Pore size distribution was analysed using Barrett–Joyner–Halenda (BJH) model. Scanning electron microscopic (SEM) images and semiquantitative EDS microanalyses were taken on a Hitachi S-3400N. Prior to the analyses, the samples were sputtered with a thin film of gold. Diffuse reflectance UV–vis (DRUV–vis) spectra of the catalyst samples were taken with a Varian Cary 100 spectrophotometer equipped with a diffuse reflectance accessory in the region 200–800 nm, with boric acid as reference. The reflectance spectra were converted into Kubelka–Munk function ($F(R)$) which is proportional to the absorption co-efficient for low values of $F(R)$. Photoluminescence spectra were recorded with Hitachi F-4500 spectrofluorimeter. Temperature programmed desorption profiles were obtained on CHEMBET 3000 (Quantachrome, USA). About 0.05 g of the sample was housed in between the quartz U-tube. Prior to analysis, the samples were degassed at 250 °C for 1.5 h under N_2 flow (80 ml/min). It was cooled down to 40 °C. The samples were saturated with NH_3 by the flow of 20% NH_3/balanced He for 30–40 min (80 ml/min). The N_2 gas was flowed over catalyst (80 ml/min) for 30 min to remove the NH_3 which might be present on the surface. The temperature was increased from 40 to 850 °C with the flow of N_2 (80 ml/min) to get a TPD profile. The amount of NH_3 consumed was determined by TCD detector by comparing the peak area of TPD with that of the peak area of known amount of ammonia under pulse titration process. X-ray photoelectron spectroscopy (XPS) measurements were performed on a VG Microtech Multilab ESCA 3000 spectrometer with a nonmonochromatised Mg-Kα X-ray source. Energy resolution of the spectrometer was set at 0.8 eV with Mg-Kα radiation at pass energy of 50 eV. The binding energy correction was performed using the C 1s peak of carbon at 284.9 eV as a reference. Current voltage was measured using a conventional Pyrex electrochemical cell consisted of a prepared electrode, a platinum wire as a counter electrode (1 mm in diameter, 15 mm in length), and an Ag/AgCl reference electrode. The cell was filled with an aqueous solution of 0.1 M Na_2SO_4 and the pH of the solution was adjusted to 5.9 by adding H_2SO_4. The photocurrent is maximum at pH 5.9. The electrolyte was saturated with argon prior to electrochemical measurements and the potential of the electrode was controlled by a potentiostat (HZ-5000, Hokuto Denko; SDPS-501C, Syrinx). Irradiation was performed through the conducting glass using a 300 W Xe lamp with a cold mirror and cutoff filters (Hoya) as necessary. It should be noted that the FTO (fluorine doped tin oxide) did not show photoresponse in the solution. The incident photon-to-photocurrent efficiency of the photoelectrode was examined by a monochromatic light source with a band-pass filter at 420 nm.

The photocatalytic degradation of organic pollutants was performed by taking 20 ml of 100 ppm substrate solution in 100 ml triple walled Pyrex batch reactor containing 1 g/L of catalyst. A solution of 2 M $NaNO_2$ was filled in the middle chamber to filter out UV light from the solar light ($\lambda \geq 400$ nm) (Scheme 1). The solutions were exposed to sunlight (central wavelength 556 nm) at room temperature (35 ± 5 °C) and agitated with magnetic stirrer to get ensured that all the active sites of catalysts are in contact with the dye solution and exposed to solar light. All the experiments were performed in triplicate during the month of April and May (sunny days) from 11.00 a.m. to 3.00 p.m. The photocatalytic experiments under sunlight were compared with the dark reactions. The quantitative analysis of the dyes and phenol [26] was done at various λ_{max} values by UV–vis spectrophotometer (Cary 1E, Varian). The control experiments were carried out under similar parametric conditions with dye solutions in the absence of catalyst to know the extent of photolysis. The light intensity was measured by Digital Illuminance Meter (TES-1332A, Taiwan) with inbuilt Si-diode. The average light intensity was around 67,500 lx, which was nearly constant during the experiments.

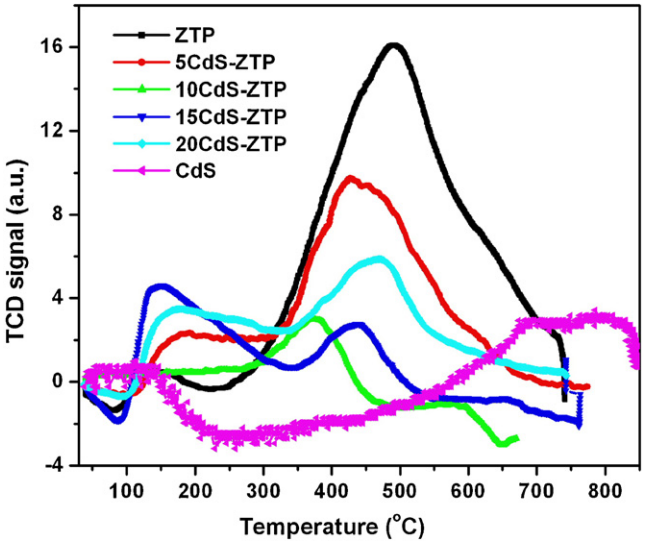

Fig. 1. Temperature programmed desorption (TPD) of *x*CdS-ZTP.

3. Results and discussion

3.1. Physical properties

The most part of the characterizations were explained elsewhere by the same authors [23]. It was observed that the pillared materials are mesoporous in character which is showing a diffraction peak at $2\theta = 0.8°$. The mesoporousity was also supported by N_2 adsorption–desorption studies which is reported elsewhere [23]. The interaction of CdS with the layers is very well evidenced from X-ray photoelectron spectra. The binding energy corresponding to Cd $3d_{5/2}$ and $3d_{3/2}$ was found to shift towards higher values i.e. from 399 eV to 404.5 and 411.4 eV, respectively. This shift of binding energy suggests some chemical interaction between the Cd^{2+} and ZTP [23]. The aforementioned characterizations were again supported in Fig. 1 and Table 1. It is very clear from the table that the acid sites were decreased from 3.4 to 0.6 mequiv./g as the basic CdS is getting inserted inside the layer of ZTP. In order to justify the statement of basicity of CdS, NH_3-TPD experiment was performed and the acidity is quite negligible i.e. 0.12 mequiv./g. A normalized plot was also given for the comparison of surface area and acid sites at various wt.% loading of CdS onto the ZTP support (Fig. 2).

Fig. 3 depicts the current–voltage curves of 15CdS-ZTP electrodes under UV irradiation as well as visible light irradiation. Anodic photocurrent was clearly observed for the electrode and exhibited highest photocurrent of 0.016 mA/cm^2 at 0.95 V vs. Ag/AgCl. The presence of anodic photocurrent indicates that the photocatalysts are n-type semiconductors [24].

Table 1
Textural characterizations results of *x*CdS-ZTP.

Sample	BET surface area (m^2/g)	Pore volume (cm^3/g)	Pore width (nm)	Acid sites[a] (mequiv./g)	CdS (wt.%)[b]
0CdS-ZTP	102	0.55	4.0	3.4	0
5CdS-ZTP	115	0.56	8.1	1.2	3.5
10CdS-ZTP	128	0.34	3.0	1.1	6.6
15CdS-ZTP	135	0.48	3.1	0.8	10.2
20CdS-ZTP	57	0.37	3.1	0.6	10.5
CdS	–	–	–	0.12	–

[a] Calculated from NH_3-TPD.
[b] Determined from EDS analysis.

3.2. Photocatalytic properties

The photodegradation of methylene blue was studied over various wt.% of CdS intercalated ZTP (Fig. 4). With increase in the wt.% of CdS, the percentage of photodegradation increases from 76 to 85% and with further increase in loading to 20 wt.%, activity decreases to 65%. This might be due to increase in surface area of 15CdS-ZTP (135 m^2/g) which enhances the adsorption of MB and subsequently the degradation. In case of 20CdS-ZTP, the surface area was observed to be drastically low i.e. 57 m^2/g which inhibits adsorption efficiency and hence photodegradation.

On the other hand, the higher activity of 15CdS-ZTP can also be explained on the basis of charge transfer within the semiconductor. Significant PL quenching was observed in case of 15CdS-ZTP which suggests the efficient charge transfer within the said semiconductor [23].

To understand the activity of the semiconductor towards the degradation of organic pollutants, phenol degradation was also performed as a model reaction. Although the rate of phenol degradation was found to be less as compared to other dyes especially MB which is studied extensively in the present investigation, but still the phenol degradation was found to be highest *ca.* 64% over 15CdS-ZTP (Fig. 4). The filtrate was subjected to atomic absorption spectroscopy (AAS) and leaching of CdS was not noticed.

Several cationic and anionic dyes were subjected to photocatalytic degradation over 15CdS-ZTP. It was observed that the cationic dyes like methylene blue (MB), malachite green (MG) and methyl violet (MV) show highest percentage of degradation as compared to anionic dye eosin B (EB) over catalyst under solar light illumination (Fig. 5). This might be due to the fact that the surface of CdS-ZTP is negatively charged which attract more number of cationic dyes results in high activity. Similar observations were observed by Rauf and Ashraf over titania under UV light [27].

On the other side, amongst the cationic dyes, the percentage of degradation of methylene blue is less as compared to methyl violet and malachite green. This could possibly be due to its compact anthracene structure as compared to MV and MG. But as described in the literatures, MB is generally used as a probe contaminant to evaluate the activity of photocatalysts due to its higher stability against degradation in natural conditions. Henceforth, we have used MB as representative dye under different parametric conditions over 15CdS-ZTP.

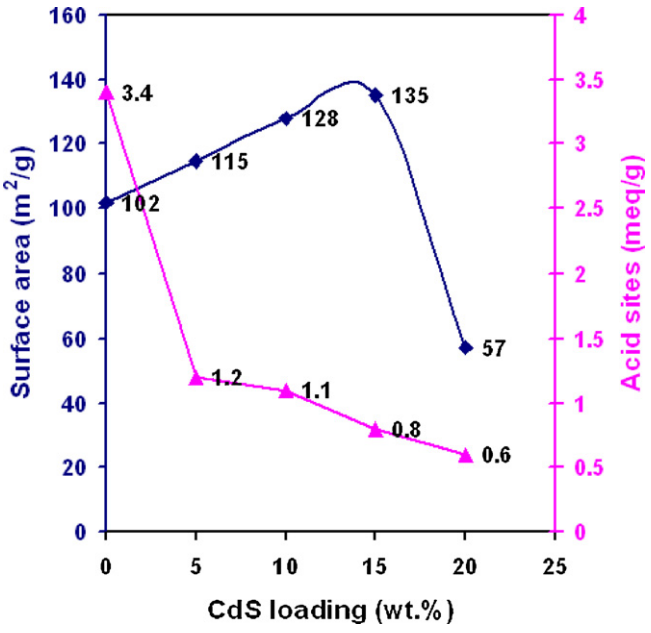

Fig. 2. Normalized plot for the comparison of surface area and acid sites as a function of CdS loading onto ZTP.

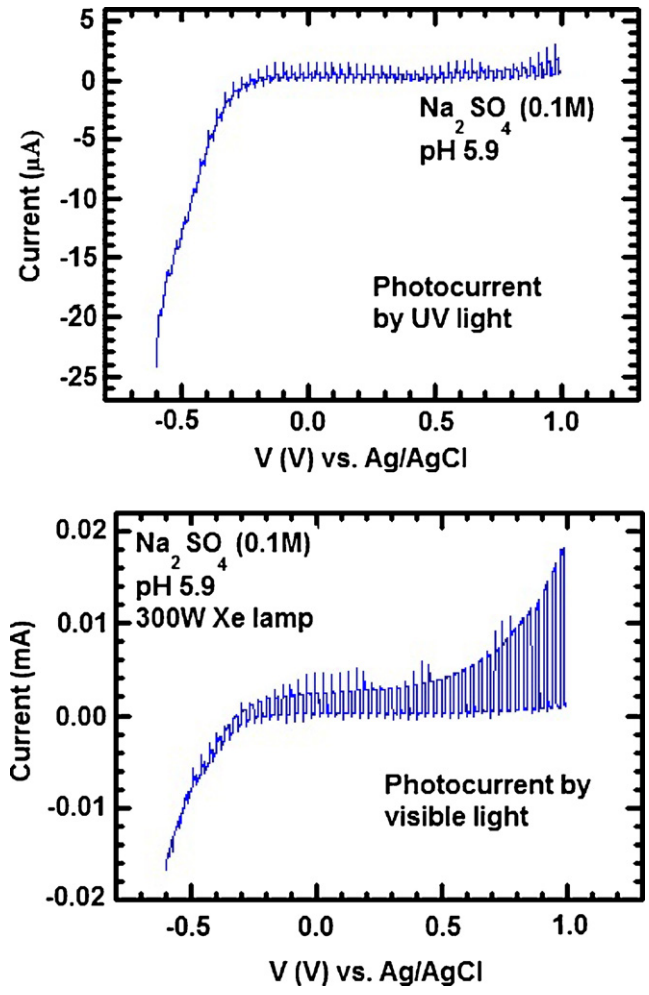

Fig. 3. Current voltage curves for 15CdS-ZTP electrodes under UV (>300 nm) and visible (>420 nm) irradiation in 0.1 M Na_2SO_4 (pH 5.9).

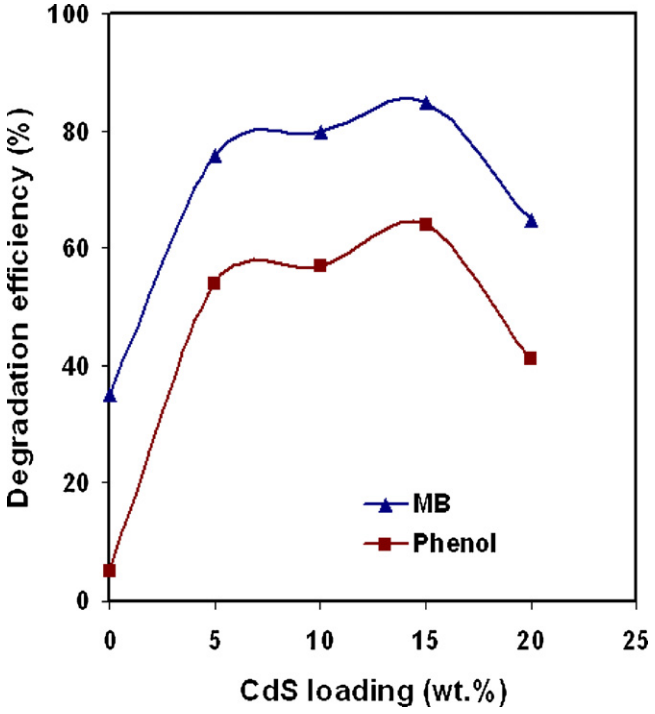

Fig. 4. Effect of CdS loading on the activity of *x*CdS-ZTP towards photodegradation of methylene blue and phenol. [MB]/[phenol] = 100 mg/L; [*x*CdS-ZTP] = 1 g/L; time = 180 min.

MB degradation as a function of catalyst concentration was investigated over 15CdS-ZTP. Fig. 6 shows an enhancement of photodegradation of MB with increase in the catalyst concentration up to 1 g/L i.e. 85% and thereafter it remained constant. The MB concentration remaining constant, the increase of catalyst concentration after 1 g/L may not be affecting the degradation of MB. Some authors reported the negative effect on the percentage of degradation of reactive dyes at higher catalyst concentration [28]. Our observation agrees with the observation reported by Sauer et al. [29] for degradation of Safira dye using Degussa P-25 and Das et al. [30] over titania pillared ZrP and TiP for the degradation of MB under solar radiation. Fig. 7 reveals the temporal evolution of the

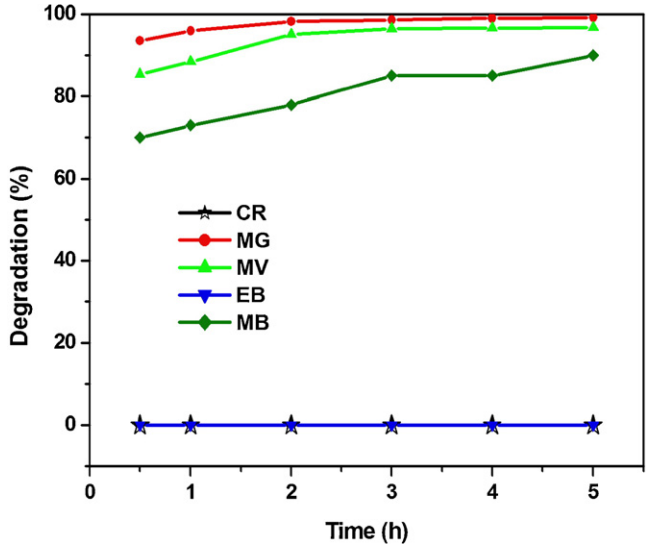

Fig. 5. Comparison of various dye degradation over 15CdS-ZTP as a function of time of irradiation. [Dye] = 100 mg/L; [15CdS-ZTP] = 1 g/L.

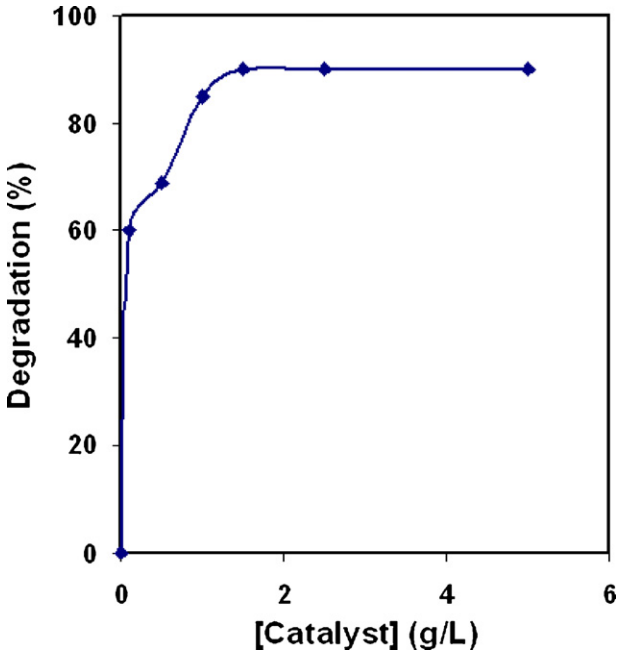

Fig. 6. Effect of catalyst concentration on MB degradation over 15CdS-ZTP. [MB] = 100 mg/L; irradiation time = 180 min.

absorption spectra of an MB aqueous solution catalysed by the 15CdS-ZTP under solar light. A gradual decrease of MB absorption under solar light illumination is observed, accompanied with an absorption band shift to shorter wavelengths. This hypsochromic shift may be attributed to the oxidized dye products. In addition, the color of the dye solution changes from deep blue to transparent light blue, which can be observed by the naked eye indicating the complete photocatalytic decolorisation of MB aqueous solution during the reaction.

We have studied the effect of initial concentration of MB on photodegradation process (Fig. 8). MB was completely decolorised at lower concentration i.e. 20–50 mg/L. In general, with increase in concentration from 20 to 150 mg/L, the percentage of degradation of MB decreases from 100 to 46%. This could possibly be due to the fact that with increase in the concentration of MB, the light absorbed by the substrate is more as compared to the

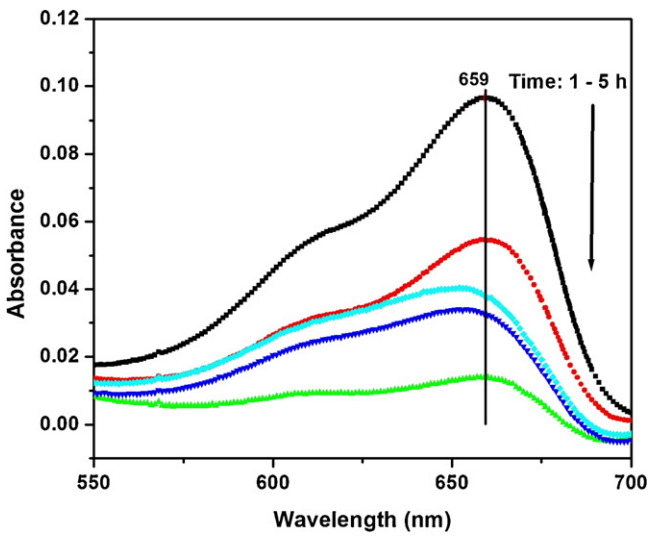

Fig. 7. Temporal evolution of the absorption spectra of MB solution under solar light illumination.

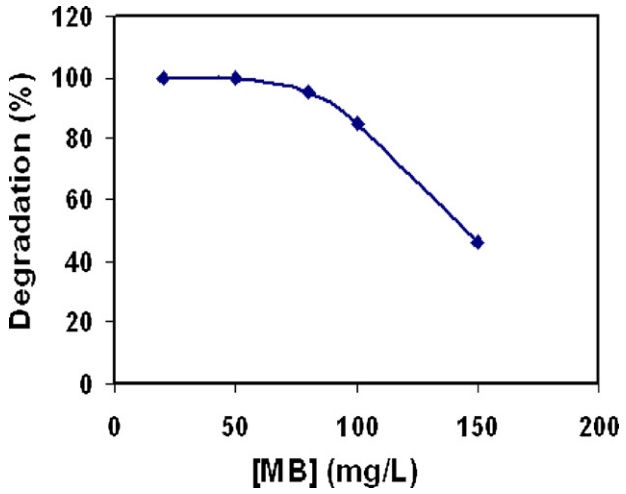

Fig. 8. Effect of initial concentration on photodegradation of methylene blue [15CdS-ZTP] = 1 g/L; time = 180 min.

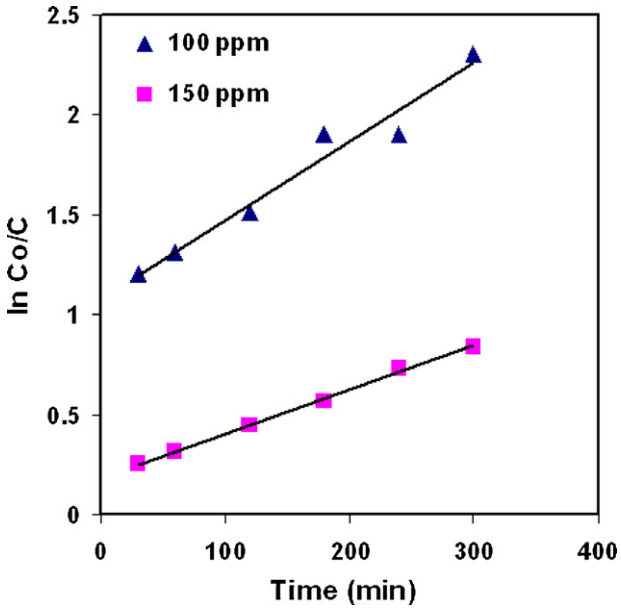

Fig. 9. Plot of log Co/*C* vs. irradiation time for MB degradation [15CdS-ZTP = 1 g/L], pH 6.5.

catalyst, which is ineffective in bringing about the photodegradation. So, at higher concentration, the percentage of photodegradation decreases.

It is known that MB can absorb the whole range of visible light, which is attributed to the ground state (MB) and the excited state (MB*) of the dye. Therefore, *x*CdS-ZTP and MB are both capable of absorbing light. Since, we are carrying out the degradation process under solar light illumination and the central wavelength is 556 nm, MB was the main material absorbing light irradiation. In the present experimental condition, photolysis[1] of MB is not possible (as was observed from Fig. 6). So, *x*CdS-ZTP played an important role in the photocatalytic decomposition of MB even if the light wavelength is ≥556 nm. When $\lambda \geq 556$ nm, MB absorbed the incident photon flux and the photogenerated electrons were transferred from ground state to the excited state of the dye owing to intramolecular π–π^* transition, then the photoelectrons of excited state were immediately injected into conduction band of *x*CdS-ZTP. Subsequently, the photoelectrons in the conduction band were captured by O_2 dissolved in water and the oxidized dyes were degraded via several intermediates.

The variation of initial concentration in the range of 100–150 mg/L on the photodegradation of MB was studied under normal pH over 1 g/L of catalyst. Photodegradation of MB was observed to follow pseudo first-order kinetics with Langmuir–Hinshelwood mechanism (Eq. (1)) over 15CdS-ZTP.

A linear relationship was observed between MB concentration and irradiation time as shown in Fig. 9 [ln Co/*C* vs. time, where Co = initial concentration of MB and *C* = concentration of MB at time *t*]. The calculated apparent rate constants "k_{app}" at different MB concentrations was given in Table 2. The rate constant value was found to decrease with increase in the MB concentration.

$$-\ln\left(\frac{C}{Co}\right) = k_{app}t \quad (1)$$

Table 2
Rate constant values for photodegradation of MB.

Time (min)	ln Co/*C*	
	100 mg/L	150 mg/L
30	1.20	0.26
60	1.31	0.32
120	1.51	0.45
180	1.9	0.57
240	1.9	0.734
300	2.303	0.844
Apparent rate constant, k_{app} (min^{-1})	0.01693	0.004466

After the 1st run, the catalyst was recovered by several washings, centrifugation and activation at 350 °C for 2 h to remove the remaining MB from the surface. The experiments were carried out under similar conditions taking the recovered catalyst. It was observed that there is no change in the activity of the catalyst up to 5 runs.

The mechanism concerning MB degradation, Cd^{2+} is the vacancy doping onto ZTP matrix for which a new conduction band might be forming below the original one for which the system acquire a metallic electronic property as a consequence of which the transition of electron is easier.

$$CdS + h\nu \rightarrow CdS\ (h^+ + e^-) \quad (2)$$

$$ZTP + h\nu \rightarrow ZTP\ (h^+ + e^-) \quad (3)$$

$$CdS\ (h^+ + e^-) + ZTP \rightarrow CdS\ (h^+)ZTP\ (e^-) \quad (4)$$

$$CdS\ (h^+ + e^-) + ZTP\ (h^+ + e^-) \rightarrow CdS\ (h^+ + h^+) + ZTP\ (e^- + e^-) \quad (5)$$

$$e^- + O_2 \rightarrow {}^\bullet O_2^- \quad (6)$$

$$H^+ + OH^- \rightarrow {}^\bullet OH \quad (7)$$

$$MB + {}^\bullet OH \rightarrow CO_2 + H_2O + NH_4^+ + NO_3^- + SO_4^{2-} + Cl^- \quad (8)$$

In order to get some information about the degradation mechanism of methylene blue over CdS-ZTP, possible pathway of the photoelectrons transfer excited by sunlight illumination was systematically investigated. It was observed that 15CdS-ZTP showed

[1] MB can be decolorised via oxidation by holes of valence band into $MB^{\bullet+}$ ($E^0_{MB^{\bullet+}/MB} = 1.08$ V), by reduction into $MB^{\bullet-}$ by conduction band electrons ($E^0_{MB/MB^{\bullet-}} = -0.23$ V) followed by $MB^{\bullet-}$ disproportionation into *leuco*-MB ($E^0_{MB/LMB} \approx 0$ V) even in the presence of aerobic conditions or without catalyst by light illumination as was reported by Mrowetz et al. [31]. Since the re-oxidation of *leuco*-MB to MB is a very fast process above pH 6.0 as reported by Impert et al. (the experimental pH is 6.5) [32]. Hence, the decolorisation occurring in our case is only because of the oxidation process due to valence band holes and conduction band electrons of *x*CdS-ZTP semiconductor, respectively not by self decomposition of the dye itself.

the ability of absorbing visible light shorter than 450 nm [23], which could cause the transition of electrons from valence band (VB) to the conduction band (CB) creating electron–hole pair (Eqs. (2)–(5)) [33]. Then the electrons in the conduction band were captured by O_2 dissolved in water, correspondingly the holes in the valence band react with –OH or H_2O which were adsorbed on the surface of *x*CdS-ZTP to give the hydroxyl radical (•OH) (Eqs. (6) and (7)). It was reported that the produced hydroxyl radical initiates various oxidation of methylene blue and ring breaking might be taking place forming various byproducts such as carbon dioxide, water, nitrate, sulfate and hydrochloric acids at very low concentrations (Eq. (8)).

4. Conclusion

The photocatalytic efficiency of ZTP has been enhanced by three folds by CdS pillaring. This may be due to increase in surface area, visible light absorption edge and decreasing band gap energy from 3.2 eV to 2.81 eV. The pillared materials showed excellent activity towards degradation of organic pollutants under solar light illumination. 15CdS-ZTP showed the best photoactivity in the range of 70–94% and 64% in 180 min towards the degradation of textile dyes and phenol, respectively. The process followed pseudo 1st order kinetics with Langmuir–Hinshelwood mechanism. The materials are found eco-friendly and reusable for photocatalytic degradation of organic pollutants in solar light.

Acknowledgements

Authors are very much thankful to Prof. B.K. Mishra, Director, IMMT, Bhubaneswar for giving permission to publish this work, Dr. K.R. Patil, NCL, Pune for doing XPS analyses, Dr. A.K. Mishra, IIT, Chennai for PL studies, Dr. K.S. Ramarao, IICT, Hyderabad for SAXS studies and Dr. B.P. Bag, CMC Dept., IMMT for giving us valuable suggestions. The financial assistance by Ministry of New and Renewable Energy (MNRE) is greatly acknowledged. One of the authors (NB) is very much grateful to CSIR for Senior Research Fellowship.

References

[1] W.Y. Choi, A. Termin, M.R. Hoffmann, J. Phys. Chem. 98 (1994) 13669–13679.
[2] X.Z. Li, F.B. Li, Environ. Sci. Technol. 35 (2001) 2381–2387.
[3] E. Borgarello, J. Kiwi, M. Gratzel, E. Pelizzetti, M. Visca, J. Am. Ceram. Soc. 104 (1982) 2996–3002.
[4] M. Anpo, Y. Ichibahashi, K. Takeuchi, H. Yamashita, Res. Chem. Intermed. 24 (1998) 143–149.
[5] I. Nakamura, N. Negishi, S. Kutsuna, T. Ihara, S. Soigihara, K. Takeuchi, J. Mol. Catal. A 161 (2000) 205–212.
[6] S. Sakthivel, H. Kisch, Angew. Chem. Int. Ed. 42 (2003) 4908–4911.
[7] S.U.M. Khan, M. Al-Shahry, W.B.J. Ingler, Science 297 (2002) 2243–2245.
[8] T. Ohno, T. Mitsui, M. Matsumura, Chem. Lett. 32 (2003) 364–365.
[9] T. Umebayashi, T. Yamaki, H. Itoh, K. Asai, Phys. Lett. 81 (2002) 454–456.
[10] T. Umebayashi, T. Yamaki, S. Tanaka, K. Asai, Chem. Lett. 32 (2003) 330–331.
[11] W. Zhao, W. Ma, C. Chen, J. Zhao, Z. Shuai, J. Am. Chem. Soc. 126 (2004) 4782–4783.
[12] W.Y. Choi, A. Termin, M.R. Hoffmann, Angew. Chem. Int. Ed. Engl. 33 (1994) 1091–1092.
[13] A. Kudo, M. Sikizawa, Catal. Lett. 58 (1999) 241–243.
[14] A. Kudo, I. Tsuji, H. Kato, Chem. Commun. (2002) 1958–1959.
[15] Z.B. Lei, G.J. Ma, M.Y. Liu, W.S. You, H.J. Yan, G.P. Wu, T. Takata, M. Hara, K. Domen, C. Li, J. Catal. 237 (2006) 322–329.
[16] D. Meissner, R. Memming, B. Kastening, J. Phys. Chem. 92 (1988) 3476–3483.
[17] T.R. Thurston, J.P. Wilconxon, J. Phys. Chem. B 103 (1999) 11–17.
[18] C.J. Lin, Y.H. Yu, Y.H. Liou, Appl. Catal. B: Environ. 93 (2009) 119–125.
[19] H. Zhu, B. Yang, J. Xu, Z. Fu, M. Wen, T. Guo, S. Fu, J. Zuo, S. Zhang, Appl. Catal. B: Environ. 90 (2009) 463–469.
[20] A.W.H. Mau, C.B. Huang, N. Kakuta, A.J. Bard, A. Campion, M.A. Fox, J.M. White, S.E. Webber, J. Am. Chem. Soc. 106 (1984) 6537–6542.
[21] H. Fujii, M. Ohtaki, K. Eguchi, J. Mol. Catal. A 129 (1998) 61–68.
[22] G.Q. Guan, T. Kida, K. Kusakabe, K. Kimura, X.M. Fang, T.L. Ma, E. Abe, A. Yoshida, Chem. Phys. Lett. 385 (2004) 319–322.
[23] K.M. Parida, N. Biswal, D.P. Das, S. Martha, Int. J. Hydr. Ener. 35 (2010) 5262–5269.
[24] K.M. Parida, S. Martha, D.P. Das, N. Biswal, J. Mater. Chem. 20 (2010) 7144–7149.
[25] M.P. Kapoor, S. Inagaki, H. Yoshida, J. Phys. Chem. B 109 (2005) 9231–9238.
[26] E.A. Clesceri, A. Greenberg, Standard Methods For Examinations of Water and Wastewater, 19th ed., APHA, AWWA and WEF, Washington, DC, 1995.
[27] M.A. Rauf, S.S. Ashraf, Chem. Eng. J. 151 (2009) 10–18.
[28] B. Neppolian, H.C. Choi, S. Sakthivel, B. Arabindoo, V. Murugasen, J. Hazard. Mater. 89 (2002) 303–317.
[29] T. Sauer, G. Cesconeto Neto, H.J. Jose, R.F.P.M. Mareira, J. Photochem. Photobiol. A: Chem. 149 (2002) 147–154.
[30] D.P. Das, N. Baliarsingh, K.M. Parida, J. Mol. Catal. A: Chem. 261 (2007) 254–261.
[31] M. Mrowetz, W. Balcerski, A.J. Colussi, M.R. Hoffmann, J. Phys. Chem. B 108 (2004) 17269–17273.
[32] O. Impert, A. Katafias, P. Kita, A. Mills, A. Pietkiewicz-Graczyk, G. Wrzeszcz, Dalton Trans. (2003) 348–353.
[33] W. Ho, J.C. Yu, J. Lin, J. Yu, P. Li, Langmuir 20 (2004) 5865–5869.